Naproxen-Based Hydrazones as Effective Corrosion Inhibitors for Mild Steel in 1.0 M HCl

Maryam Chafiq [1], Abdelkarim Chaouiki [1], Mustafa R. Al-Hadeethi [2] , Ismat H. Ali [3] , Shaaban K. Mohamed [4,5], Karima Toumiat [6] and Rachid Salghi [1,*]

[1] Laboratory of Applied Chemistry and Environment, ENSA, University Ibn Zohr, P.O. Box 1136, Agadir 80000, Morocco; maryam.chafiq@edu.uiz.ac.ma (M.C.); abdelkarim.chaouiki@uit.ac.ma (A.C.)

[2] Department of Chemistry, College of Education, Kirkuk University, Kirkuk 36001, Iraq; mustfaa70@yahoo.com

[3] Department of Chemistry, College of Science, King Khalid University, P.O. Box 9004, Abha 61413, Saudi Arabia; ismathassanali@gmail.com

[4] Chemistry and Environmental Division, Manchester Metropolitan University, Manchester M15 6BH, UK; shaabankamel@yahoo.com

[5] Chemistry Department, Faculty of Science, Minia University, El-Minia 61519, Egypt

[6] Department of Materials Sciences, Laghouat University, P.O. Box 37, Laghouat 03000, Algeria; toumiat.k@gmail.com

* Correspondence: r.salghi@uiz.ac.ma

Abstract: The corrosion-inhibiting performance of (E)-N'-(4-bromobenzylidene)-2-(6-methoxynaphthalen-2-yl) propanehydrazide (BPH) and (E)-N'-(4-(dimethylamino) benzylidene)-2-(6-methoxynaphthalen-2-yl) propanehydrazide (MPH) for mild steel (MS) in 1.0 M HCl was investigated using electrochemical methods, weight loss measurements, and scanning electron microscope (SEM) coupled with energy dispersive X-ray spectroscope (EDX) analysis. Raising the concentration of both inhibitors towards an optimal value of 5×10^{-3} M reduced the corrosion current density (i_{corr}) and the corrosion rate of mild steel. The inhibitory effect of MPH, which showed the highest inhibition efficiency, was explored under a range of temperatures between 303 and 333 K. The inhibitory performance of both compounds significantly improved when the inhibitor concentration increased. The main result that flowed from potentiodynamic polarization (PDP) tests was that both compounds acted as mixed-type inhibitors, with a predominance cathodic effect. The adsorption of both compounds follows the Langmuir isotherm. SEM/EDX confirmed the excellent inhibition performance of tested compounds.

Keywords: corrosion inhibition; mild steel; SEM; EDX; electrochemical measurements

1. Introduction

In industry, many acidic solvents are extensively used, particularly for removing different types of locally occurring deposits such as rust or scale. Among them, chloride acid is very often used [1,2]. Contrarily, the most extensively used metal in these industrial sectors is mild steel on account of its outstanding mechanical performance, extreme thermal stability, high tensile strength, its manufacturability, and economical price [3–9]. Despite such importance, mild steel is highly susceptible to corrosion in acidic media [10]. Industrial installations and equipment that are likely to bedamagedcan be designed and built, taking into account the available anti-corrosion treatments [11–15]. The field of metal conservation has borrowed specific corrosion protection strategies. Among them are corrosion inhibitors that are now considered as one of the most reliable approaches to diminish the aggressive intervention of corrosive species on metals, and it is also

the most cost-effective [16]. When it comes to the use of inhibitors, improving the performance of environmentally friendly compounds has become an exciting new science and a challenging task for chemists and technologists today. In this frame of reference, the anti-corrosion effect of two new compounds, namely, (E)-N'-(4-bromobenzylidene)-2-(6-methoxynaphthalen-2-yl) propanehydrazide (BPH) and (E)-N'-(4-(dimethylamino) benzylidene)-2-(6-methoxynaphthalen-2-yl) propanehydrazide (MPH) are being broughtinto play in the process of inhibiting corrosion of mild steel (MS) in a 1.0 M HCl medium. The selection of such molecules was based primarily around the presence of a combination of aromatic rings, oxygen, nitrogen, and other heteroatoms, which are capable of promoting adsorption of both molecules on the surface of MS.

Naproxen has long been considered as the most effective non-steroidal anti-inflammatory drugs (NSAIDs), but because of its carboxylic group, there were some limitations. To minimize the side effects and to enhance the anti-inflammatory activity, the functionalization of the carboxylic group is acrucial step [17]. One of the most effective functionalizations of the carboxylic group is its conversion into hydrazone derivatives [18]. Hydrazones are classified as belonging to the Schiff base group. Researchers have found broad applications for it in pharmacological chemistry as an antibacterial, anticonvulsant, anticancer, antitumor and anti-inflammatory agent [19]. Hydrazones contain azomethine group R_1R_2–C=NNH_2 where R_1 and R_2 are different functional groups, meaning that hydrazones are very important starting materials in bioactive heterocycles [20]. The azomethine bond can conjugate with a lone pair of electrons of the terminal nitrogen atom. The nitrogen and carbon atoms of hydrazones have a significant role in their physical and chemical properties. Nitrogen atoms have a nucleophilic character, while the carbon atom has two characters, i.e., nucleophilic and electrophilic [21]. In addition to their biological importance, hydrazones play a vital role in the bioinorganic field because of their capability to form a stable metal chelates with all transition metals [22]. Nowadays, many trial studies have been conducted to develop corrosion inhibitors based on hydrazones derived from NSAIDs to protect a broad range of metals and alloys [23,24].

As part of this work, and as a continuation of our studies on hydrazones [23–25], we report the corrosion inhibition properties of new hydrazone-based organic molecules for MS in an acidic solution. Electrochemical impedance spectroscopies (EIS), weight loss (WL) as well as potentiodynamic polarization (PDP) were adopted as experimental methods to test the resistance of the studied metal after adding BPH and MPH to 1.0 M HCl. The gravimetric technique was implemented by modifying temperatures from 303 K to 333 K to examine the impact of temperature on the effectiveness of MPH. At the same time, the effect of immersion time is monitored by the EIS method for 24 h. The experimental results are explained in more detail by surface analysis using SEM and EDX techniques.
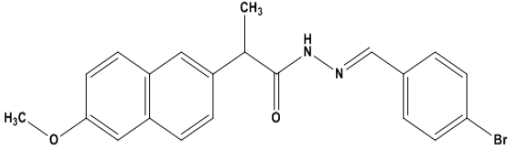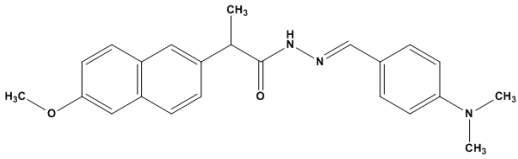
2. Materials and Methods

2.1. Materials and Electrolytes

The studies are carried out on MS, and the chemical composite of which is shown in Table 1. A hydrochloric solution at a concentration of 1.0 M prepared from a 37% HCl solution by diluting it with distilled water was used for the experimental measurements. Using a rotating disc containing 400, 800, 1200 and 1600 grit emery papers, the samples of mild steel were smoothed with the polishing machine before the application of different assays. After that, all MS specimens were degreased in acetone and rinsed using distilled water. Following this, the specimens were draught-dried. BPH and MPH were evaluated against the corrosion of mild steel (MS) with a concentration range of 1×10^{-4} to 5×10^{-3} M. Table 2 lists the molecular structure of the tested compounds along with their chemical name and abbreviation. The full synthesis and characterization details of both compounds are given in the Supplementary Material (Figure S1).

Table 1. Chemical composition of the studied mild steel (MS).

Atom	Fe	C	Si	Mn	S	Cr	Ti	Ni	Co	Cu
Content (%)	98.388	0.371	0.229	0.681	0.014	0.076	0.012	0.058	0.010	0.161

Table 2. Molecular structures of (E)-N′-(4-(dimethylamino) benzylidene)-2-(6-methoxynaphthalen-2-yl) propanehydrazide (MPH) and (E)-N′-(4-bromobenzylidene)-2-(6-methoxynaphthalen-2-yl) propanehydrazide (BPH).

Inhibitors	Names and Abbreviation
	(E)-N′-(4-bromobenzylidene)-2-(6-methoxynaphthalen-2-yl) propanehydrazide (BPH)
	(E)-N′-(4-(dimethylamino)benzylidene)-2-(6-methoxynaphthalen-2-yl) propanehydrazide (MPH)

2.2. Weight Loss (WL)

Following the ASTM G 31-72 method [26], and based on the gravimetric method, the average corrosion rate of mild steel was determined. Tests were achieved on MS in the form of rectangular pieces with a diameter of 2.4 cm × 1.9 cm and a thickness of 0.4 cm and that were soaked in 80 mL of 1.0 M HCl solution without and with the addition of inhibitors at diverse concentrations. The surface morphology of the MS was treated using emery papers of different qualities from 400 to 1600 and thoroughly cleaned. The MS samples were weighed with a precision balance and allowed to plunge into inhibitor solutions in different temperatures (303 to 333 K). The samples were immersed in triplicate. After this, they were removed and cleaned thoroughly using distilled water and acetone, air-dried and finally weighed again precisely as described above. The difference in weight loss was confirmed. For the calculation of the corrosion rate, the average mass loss was used using Equation (1) [27]:

$$C_{WL} = \frac{K \times W}{A \times t \times \rho} \tag{1}$$

From the ASTM standard methods: W referred to in the equation means the loss in mass given in units of grams; where t indicates submersion time, generally given in hours; and A is the exposed area in cm^2. $K = 8.76 \times 10^4$ was used as constant.

Equations (2) and (3) were applied when calculating the inhibitory efficacy of the tested molecules and their surface coverage, respectively.

$$\eta_{WL}(\%) = \left[1 - \frac{C_{WL}}{C^\circ_{WL}}\right] \times 100 \tag{2}$$

$$\theta = \frac{C^\circ_{WL} - C_{WL}}{C^\circ_{WL}} \tag{3}$$

Here, θ means the degree of surface coverage of BPH and MPH, C_{WL} and C°_{WL} refer to the corrosion rates of mild steel with and without concentrations of inhibitors, respectively.

2.3. Electrochemical Measurements

The electrochemical tests were conducted using a 3-electrode cell linked to a PGZ 100 type Potentiostat guided via "Voltalab Master 4" analyzer program (Version 4.0, Radiometer Analytical, Lyon, France). A saturated calomel electrode is used as the reference electrode. The auxiliary electrode (counter-electrode) is a platinum grid, and the MS electrode is used as the working electrode, which has a surface area of 1 cm^2, and is placed close to the reference electrode. Such measurements were made using a cell containing 80 mL of the solution. Preceding all these tests, the stability of the open circuit potential was monitored for 30 min. The potentiodynamic polarization measurements were carried out in an interval of −800 to −200 mV of the corrosion potential with a sweep rate of 0.16 mV s^{-1}. For the EIS measurements, the tests were conducted in a frequency range of 10 mHz to 100 kHz and an alternating amplitude of 10 mV.

For the potentiodynamic polarization study, the corresponding inhibition efficiency was estimated from current density according to the following equation:

$$\eta_{PDP}(\%) = \frac{i_{corr}^\circ - i_{corr}}{i_{corr}^\circ} \times 100 \tag{4}$$

where i_{corr}° and i_{corr} represent, respectively, the corrosion current density of mild steel in HCl solution and that in the presence of inhibitors.

Based on the EIS technique, for the determination of inhibitory efficacy, the following formula is used:

$$\eta_{EIS}(\%) = \frac{R_p^i - R_p^\circ}{R_p^i} \times 100 \tag{5}$$

where R_p° and R_p^i signify the polarization resistance in the blank and with the addition of inhibitors, respectively.

2.4. Scanning Electron Microscopy (SEM)/Energy Dispersive Spectroscopy (EDX) Studies

The analysis of specimens' surface morphology with and without an inhibitor was performed with the use of a scanning electron microscope combined with the EDX analysis. The results were achieved on samples exposed during an immersion time of 24 h in the corrosive environment and experienced the similar pre-treatment heretofore explained in the gravimetric tests. Moreover, the layers that formed on the treated steel coupons were identified and compared using an EDX analyzer adapted to the SEM.

3. Results and Discussion

3.1. Weight Loss Measurements

3.1.1. Concentration Effect

To provide an initial investigation framework related to the anti-corrosive character of the metal in an electrolyte solution, weight loss studies were employed to evaluate the inhibitory efficacy at a constant temperature of the two compounds, BPH and MPH, at different concentrations. Table 3 regroups together corrosion rate values and percentage inhibiting efficiency calculated gravimetrically for the different concentrations of BPH and MPH compounds at 303 K. Observing Table 3, it can be noted that the corrosion rate decreases and the inhibiting efficiency improves as the concentration of BPH and MPH rises, reaching a maximum value of 96.02% in the presence of 5×10^{-3} M of MPH. The results are graphically illustrated in Figure 1. MPH is highly effective against steel corrosion in the 1.0 M HCl environment, and it is more effective than BPH. The increase in inhibitory efficacy with concentration depends mainly on how strongly these inhibitors interact with the metal surface [28–30].

Both molecules are rich in heteroatoms, which facilitate their adsorption on the mild steel surface. The observed difference in the corrosion inhibition performance is a result of the difference in the functional groups present in each compound [31]. It is clear that the presence of the dimethylamino group, as a strong electro-donating group, improves the corrosion inhibition properties of MPH significantly compared to BPH that has bromide group.

Table 3. The effect of MPH and BPH concentrations on the corrosion data of MS in 1.0 M HCl.

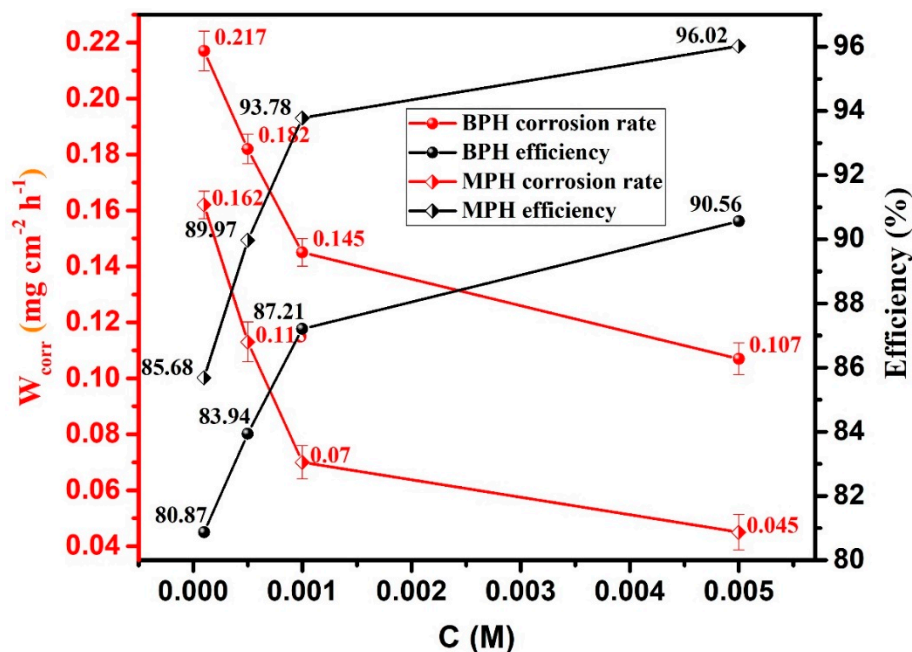| Inhibitor	Concentration (mol/L)	W (mg/(cm^2 h))	θ	η_W (%)
HCl	1	1.135 ± 0.0121	-	-
MPH	1×10^{-4}	0.162 ± 0.0049	0.85	85.68
	5×10^{-4}	0.113 ± 0.0071	0.89	89.97
	1×10^{-3}	0.070 ± 0.0059	0.93	93.78
	5×10^{-3}	0.045 ± 0.0062	0.96	96.02
BPH	1×10^{-4}	0.217 ± 0.0072	0.80	80.87
	5×10^{-4}	0.182 ± 0.0053	0.83	83.94
	1×10^{-3}	0.145 ± 0.0041	0.87	87.21
	5×10^{-3}	0.107 ± 0.0059	0.90	90.56

Figure 1. The relationship among corrosion rate, inhibition efficiency, and inhibitors concentrations for mild steel in MPH and BPH at 303 K.

3.1.2. Temperature Effect

Monitoring the temperature response to the corrosion kinetic process can provide further information regarding the MS electrochemical properties in the studied conditions. Since many inhibitor applications are carried out under different temperatures depending on the field of application of the steel, investigating the effect of temperatures on the inhibitor's efficiency would provide useful insights. The influence of temperature on the progression of the corrosion rate and the changes in inhibitory effectiveness in a temperature range of 303 to 333 K were observed. Table 4 illustrates the influence of temperature in the absence and presence of MPH, while the resulting activation parameters related to the effect of temperature are shown in Table 5.

Table 4. The effect of temperature on inhibition efficiency and the corrosion rate of MPH.

Solution	Concentration	Temperature (K)	Corrosion Rate (mg/(cm²·h))	Inhibition Efficiency (%)
Blank	1.0 M HCl	303	1.1350 ± 0.0121	-
		313	1.4162 ± 0.0215	-
		323	1.9981 ± 0.0214	-
		333	2.5392 ± 0.0316	-
MPH	1×10^{-4} M	303	0.162 ± 0.0049	85.68
		313	0.219 ± 0.0077	84.50
		323	0.319 ± 0.0079	84.01
		333	0.420 ± 0.0011	83.44
	5×10^{-4} M	303	0.113 ± 0.0071	89.97
		313	0.178 ± 0.0055	87.42
		323	0.277 ± 0.0079	86.11
		333	0.386 ± 0.0038	84.78
	1×10^{-3} M	303	0.070 ± 0.0059	93.78
		313	0.110 ± 0.0049	92.21
		323	0.176 ± 0.0081	91.19
		333	0.244 ± 0.0090	90.36
	5×10^{-3} M	303	0.045 ± 0.0062	96.02
		313	0.082 ± 0.0059	94.14
		323	0.138 ± 0.0021	93.08
		333	0.214 ± 0.0064	91.55

Table 5. Corrosion kinetic parameters for mild steel in 1.0 M HCl in the presence and absence of MPH.

Parameters	Blank	MPH			
		1×10^{-4} M	5×10^{-4} M	1×10^{-3} M	5×10^{-3} M
E_a (kJ mol⁻¹)	23.12	27.12	34.66	35.41	43.66
ΔH_a (kJ mol⁻¹)	20.48	24.48	32.03	32.77	41.02
ΔS_a (J mol⁻¹ K⁻¹)	−176.48	−167.07	−157.27	−158.83	−135.14
$E_a - \Delta H_a$ (kJ mol⁻¹)	2.64	2.64	2.63	2.64	2.64

As the temperature rises, the surface has the highest corrosion rate values. Additionally, calculated thermodynamic parameters can be derived to produce a qualitative picture of the inhibitor under investigation in the HCl solution. Using both the Arrhenius equation and the transition state functions, we have calculated the values of the kinetic parameters such as apparent entropy (ΔS_a), activation energy (E_a) and the enthalpy (ΔH_a) of activation, and these formulas were described as follows [31]:

$$C_{WL} = K \times e^{\frac{-E_a}{RT}} \tag{6}$$

$$C_{WL} = \frac{RT}{Nh} \exp\left(\frac{\Delta S_a}{R}\right) \exp\left(\frac{\Delta H_a}{RT}\right) \tag{7}$$

where K denotes the pre-exponential factor, h signifies the Planck constant, N denotes the number of Avogadro, R is the universal gas constant, and T indicates the temperature.

Figure 2 represents the Arrhenius and transition state plots, which relate the logarithm of corrosion rate as a function of the inverse of the relative temperature and ln C_{WL}/T as a function of $1/T$ with and without inhibitors. Referring to Table 5, it is indicated that the calculated values of activation energy (E_a) in the inhibited acids strongly depend on the inhibitor concentrations and arehigher than those of the blank solution. In turn, the positive enthalpy values demonstrate that MS dissolution is endothermic [3]. Concerning ΔS_a value, it could be observed that the ΔS_a is higher by comparison with

that in uninhibited solution, and it is negative. This concludes that there is less disorder or randomness present during the switch from reagents to the activated complex [32].
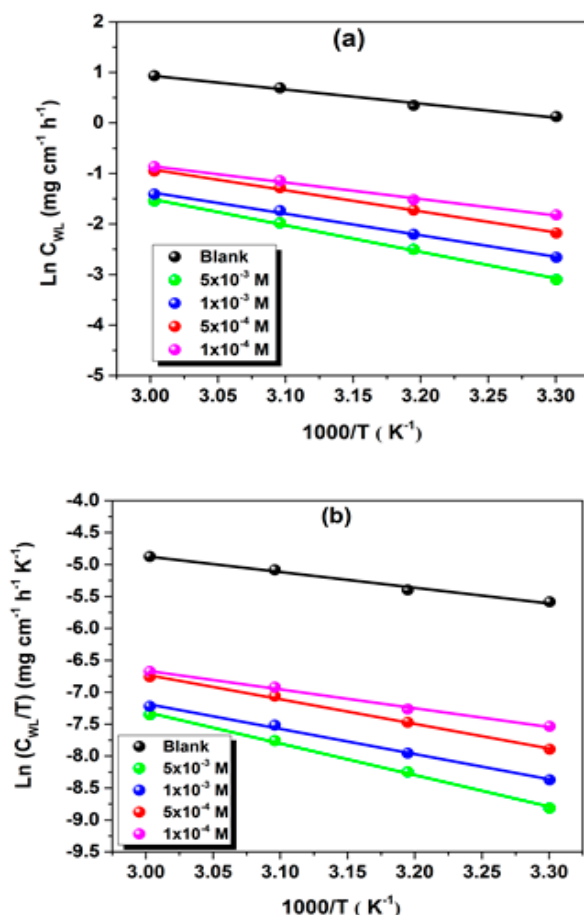

Figure 2. Arrhenius (**a**) and transition state (**b**) plots for corrosion inhibition of mild steel in the absence and presence of different concentrations of MPH in 1.0 M HCl.

3.2. Potentiodynamic Polarization (PDP) Study

To assess the corrosion performance of investigated inhibitors by interpretation of the kinetics of the anodic and cathodic reactions of the corrosion process, potentiodynamic polarization (PDP) was studied in detail. After 30 min of immersing the MS in the acid solution, The PDP curves in the absence and the presence of various concentrations of two investigated inhibitors were taken, and they are presented in Figure 3. The corrosion properties of the studied systems in terms of corrosion potential, corrosion current density (i_{corr}), Tafel slopes and corrosion rate (CR) were established and tabulated in Table 6.

The addition of BPH and MPH compounds results in a decrease in cathodic and anodic current densities with a wide range of linearity, indicating that Tafel's law is correctly verified [33]. Assuming these polarization plots, it should be noted that the occurrence of log i = f (E) versus concentration is essentially the same for the two studied inhibitors, a result that is probably caused by the immutable mechanism of the corrosion process [34]. This means that the tested inhibitors adsorbed on the surface [35], then delayed the development of cathodic hydrogen and suppressed the active dissolution of the anode metal without changing the dissolution mechanism, which is what mixed-type inhibitors are characterized by [35]. The results in Table 6 show that the addition of different concentrations of BPH and MPH to the HCl solution leads to a significant decrease in the corrosion current density and the corrosion rate of mild steel. For instance, in the case of MPH, the i_{corr} value of mild steel decreases from 0.564 mA/cm^2 (corrosion rate of 6.64 mm/y) in an uninhibited solution to 0.026 mA/cm^2 (corrosion rate of 0.31 mm/y) in the presence of 5×10^{-3} M of MPH. In addition, the inhibition efficiency values

reach 95.37% for MPH and 89.20% for BPH at 5×10^{-3} M of inhibitors. Thus, it can be concluded that hydrazone derivatives have promising corrosion resistance in the test medium. These results are consistent with those from weight loss measurements.
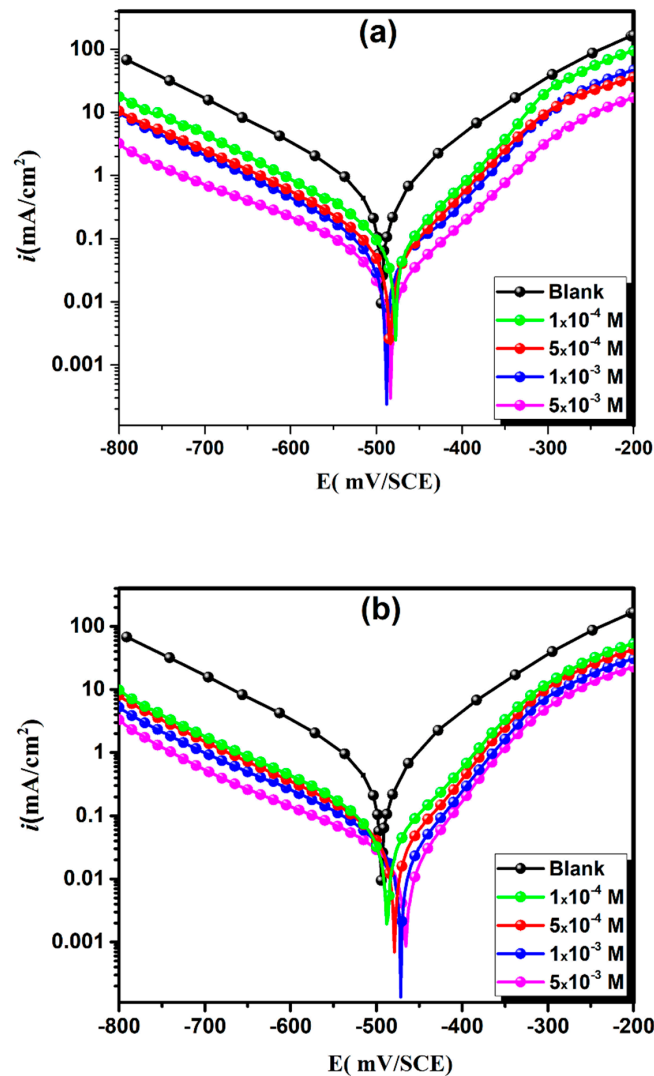

Figure 3. Potentiodynamic polarization curves of MS in hydrochloric acid solution in the presence and absence of various concentrations of BPH (**a**) and MPH (**b**) at 303 K.

Table 6. Electrochemical parameter values estimated according to potentiodynamic polarization curves of MS in hydrochloric acid solution in the presence and absence of various concentrations of MPH and BPH at 303 K.

Inhibitor	Concentration (M)	$-E_{corr}$ (mV vs. SCE)	$-\beta c$ (mV dec^{-1})	i_{corr} (mA cm^{-2})	CR (mm yr^{-1})	θ	η_{PDP} (%)
Blank	1.0	496.0 ± 0.4	162.0 ± 4.1	0.5640 ± 0.0023	6.64	-	-
MPH	1×10^{-4}	488.8 ± 1.3	162.7 ± 4.4	0.0887 ± 0.0049	1.04	0.84	84.27
	5×10^{-4}	480.3 ± 0.2	168.7 ± 7.1	0.0617 ± 0.0059	0.73	0.89	89.06
	1×10^{-3}	471.8 ± 0.9	169.2 ± 5.6	0.0424 ± 0.0056	0.50	0.92	92.48
	5×10^{-3}	467.2 ± 0.8	180.3 ± 6.1	0.0261 ± 0.0018	0.31	0.95	95.37
BPH	1×10^{-4}	481.2 ± 0.7	138.1 ± 8.3	0.1115 ± 0.0046	1.31	0.80	80.23
	5×10^{-4}	484.3 ± 0.6	142.7 ± 1.2	0.0878 ± 0.0086	1.03	0.84	84.43
	1×10^{-3}	489.8 ± 0.9	143.9 ± 7.6	0.0767 ± 0.0019	0.90	0.86	86.40
	5×10^{-3}	484.9 ± 1.1	201.5 ± 6.7	0.0609 ± 0.0066	0.72	0.89	89.20

3.3. Electrochemical Impedance Spectroscopy (EIS)Study

3.3.1. Concentration Effect

To corroborate the obtained results from the polarization curve and gain insights into the corrosion mechanisms, EIS measurements were carried out in the absence and presence of inhibitors. Both Nyquist diagrams (Figure 4a,b) and Bode representation (Figure 4c,d) of the metal are shown in Figure 4, in blank solution and the presence of BPH and MPH inhibitors at different concentrations. Further, the electrical double layer capacitance (C_{dl}) for each case was calculated by the following equation [34]:

$$C_{dl} = \sqrt[n]{Q \cdot R_p^{1-n}} \tag{8}$$

where n denotes the phase shift and estimates the surface heterogeneity of the mild steel.
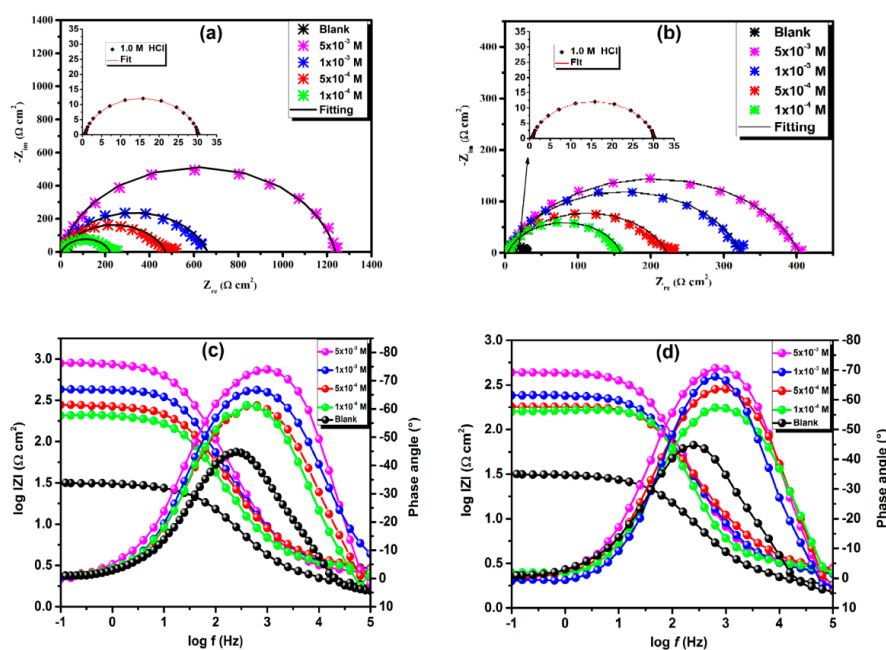

Figure 4. Nyquist and Bode diagrams of mild steel in 1.0 M HCl with and without various concentrations: (**a**,**c**) MPH and (**b**,**d**) BPH.

A summary of the values extracted from figures, i.e., R_p, C_{dl}, CPE, n, R_s and η_{EIS} can be found in Table 7. The resulting impedance curves represent a capacitive loop with increasing size as the inhibitor concentration increases due to the charge transfer process. EIS spectra with the equivalent circuit exposed in Figure 5 were adjusted to obtain R_p values significant for corrosion resistance. In previous works, the reason for using polarization resistor as an alternative to the charge transfer resistor is discussed [36,37].

It was found that with the addition of two inhibitors, the values of polarization resistance showed continuous improvement and increased with increasing concentration of the organic compounds. In contrast, the values of C_{dl} were significantly decreased. Consequently, there is a modification of the metal/electrolyte interface by a substantial increase in thickness of the electrical double layer due to the adsorption of a large number of molecules on the surface of the MS. It was noted that for both of the used inhibitors, the values of the phase angle were always higher in comparison to the blank, but were significantly far from $-90°$, which is indicative of the non-ideal capacitor [38]. As a conclusion, comparing the inhibitory efficiencies measured using the gravimetric method and the electrochemical methods (polarization curves and EIS) reveals an excellent correspondence.

Table 7. Electrochemical parameter values estimated according to electrochemical impedance spectroscopy curves of MS in HCl solution in the presence and absence of several concentrations of MPH and BPH at 303 K.

| Inhibitor	Concentration (M)	$-E_{corr}$ (mV vs. SCE)	$-\beta c$ (mV dec^{-1})	i_{corr} (mA cm^{-2})	θ	η_{PDP} (%)
Blank	1.0	496.0 ± 0.4	162.0 ± 4.1	0.5640 ± 0.0023	-	-
MPH	1×10^{-4}	488.8 ± 1.3	162.7 ± 4.4	0.0887 ± 0.0049	0.84	84.27
	5×10^{-4}	480.3 ± 0.2	168.7 ± 7.1	0.0617 ± 0.0059	0.89	89.06
	1×10^{-3}	471.8 ± 0.9	169.2 ± 5.6	0.0424 ± 0.0056	0.92	92.48
	5×10^{-3}	467.2 ± 0.8	180.3 ± 6.1	0.0261 ± 0.0018	0.95	95.37
BPH	1×10^{-4}	481.2 ± 0.7	138.1 ± 8.3	0.1115 ± 0.0046	0.80	80.23
	5×10^{-4}	484.3 ± 0.6	142.7 ± 1.2	0.0878 ± 0.0086	0.84	84.43
	1×10^{-3}	489.8 ± 0.9	143.9 ± 7.6	0.0767 ± 0.0019	0.86	86.40
	5×10^{-3}	484.9 ± 1.1	201.5 ± 6.7	0.0609 ± 0.0066	0.89	89.20
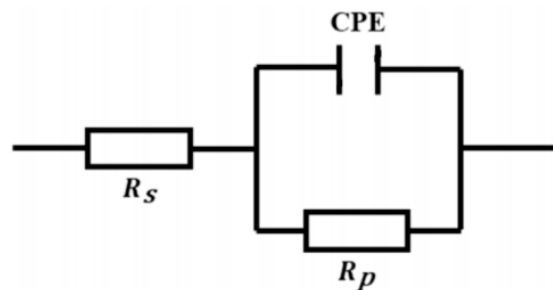
Figure 5. The equivalent circuit model applied to fit and simulate the impedance data.

3.3.2. Immersion Time Effect

As a result of recognizing the importance of immersion time in the process of inhibitor adsorption on the metal surface and its significant effect on inhibitory efficacy, curves displaying EIS plots of MPH as a function of immersion time were performed (Figure 6).
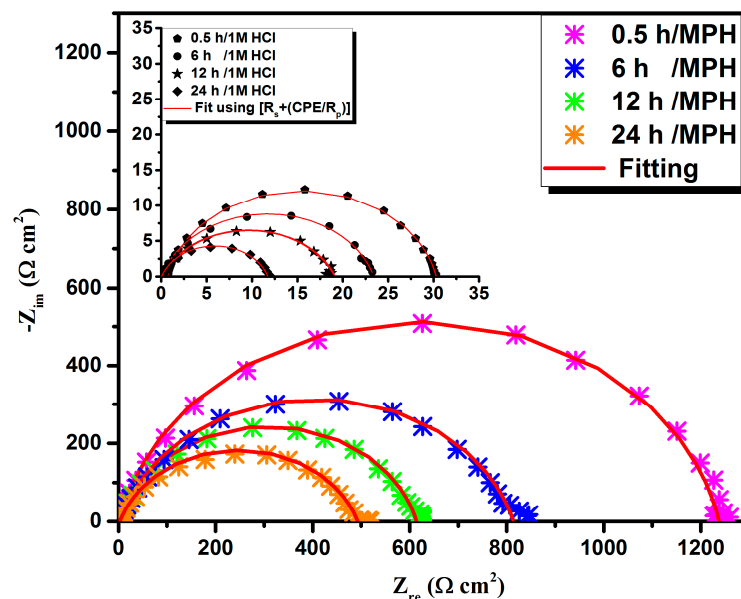

Figure 6. Electrochemical impedance spectroscopy curves of MS substrate immersed in 1.0 M HCl solution without and with 5×10^{-3} M of MPH at various times.

The improvement in inhibitory efficacy and calculated parameters are grouped in Table 8. Electrochemical impedance tests were conducted in 1.0 M HCl, with and without the compound under study, after different immersion times (30 min, 6 h, 12 h, and 24 h), at 303 K. According to Figure 6, we notice the appearance of a single capacitive loop at all tested immersion times. The polarization resistance of MS in the presence of 5×10^{-3} M of MPH decreases as the immersion time increases. However, the results in Table 8 show that the inhibition efficiency of MPH remains almost unchanged up on increasing the immersion time. This is mainly due to the number of unoccupied sites [39,40]. At the first exposure of the steel in the inhibited environment, the sites are unoccupied. Therefore the attractive forces between the surface vaccination cases and the free electrons of the heteroatom molecules will occur, which contributes to improving the efficiency during the immersion time until complete filling; in this case, the efficiency reaches a nearly constant value.

Table 8. Electrochemical impedance spectroscopy parameters for mild steel in the absence and presence of MPH vs. immersion time.

Inhibitor	Time (h)	R_p (Ω cm^2)	n	$Q \times 10^{-4}$ (S^n Ω^{-1} cm^{-2})	C_{dl} (μF cm^2)	θ	η_{EIS} (%)
Blank	0.5	29 ± 1.5	0.89 ± 0.005	1.7610 ± 0.0025	92	-	-
	6	23 ± 2.5	0.84 ± 0.007	2.5114 ± 0.0037	94	-	-
	12	18 ± 1.7	0.83 ± 0.004	2.9866 ± 0.0084	102	-	-
	24	12 ± 2.9	0.88 ± 0.003	3.0891 ± 0.0031	144	-	-
MPH	0.5	1235 ± 1.7	0.83 ± 0.009	0.1472 ± 0.0043	6.47	0.97	97.62
	6	811.3 ± 1.9	0.82 ± 0.003	0.2257 ± 0.0022	9.33	0.97	97.16
	12	610.9 ± 2.0	0.80 ± 0.011	0.3493 ± 0.0059	13.35	0.97	97.05
	24	490.0 ± 1.7	0.78 ± 0.013	0.6433 ± 0.0091	24.26	0.97	97.55

3.4. Adsorption Isotherm

The most common mechanism for inhibitory molecules is adsorption. For this reason, it is possible to confirm the adsorption behavior of the examined molecule by adapting the achieved outcomes to many known adsorption isotherms. Different types of adsorption isotherms, namely, Langmuir, Freundlich, Temkin and Frumkin, are tested to give more details on the corrosion inhibition mechanism by providing information on the interaction of the inhibitor molecules with the MS surface. In this study, among the isothermal models mentioned above, we note at this point that we obtained the closest fit from the Langmuir model. We base this result on the value of the linear regression coefficient, R^2, being close to 1 [41]. Moreover, the Langmuir isotherm describes the adsorption of the studied inhibitors onto the MS surface on the assumption of equivalent surface coverage of both homogeneous surface and active sites. The equation of the Langmuir isotherm model is as follows [41]:

$$\frac{C}{\theta} = \frac{1}{K_{ads}} + C \tag{9}$$

in which C signifies the inhibitor concentration, K_{ads} means a constant of adsorption equilibrium while θ denotes the area coverage.

The values of the adsorption coefficient (K_{ads}), estimated by extrapolating the lines obtained previously, then allowed us to access the values of the standard free adsorption energies (ΔG°_{ads}) from the Van't Hoff equation [42]:

$$K_{ads} = \frac{1}{55.5} \times exp\left(-\frac{\Delta G^{\circ}_{ads}}{RT}\right) \tag{10}$$

In the above equation, 55.5 points to the water molar concentration measured in mol L^{-1}, *T* indicates the temperature of the aqueous solution and R is known as the universal gas constant. The adsorption parameters ΔH°_{ads} and ΔS°_{ads} on the MS surface are computed according to the following relationship [43]:

$$\Delta G^{\circ}_{ads} = \Delta H^{\circ}_{ads} - T\Delta S^{\circ}_{ads} \tag{11}$$

A diagram of *C*/θ vs. *C* is given in Figure 7a. The thermodynamic parameters estimated from Langmuir's plot are tabulated in Table 9. Observing Table 9, there are high K_{ads} values, which showed significant adsorption of both inhibitors to the surface of the MS [44–47]. According to the results, using the Δ*G* values, it was confirmed that the surface was bound to the molecules by chemical and physical exchanges know as mixed adsorption. The values of ΔG°_{ads} of MPH were determined at various temperatures (Figure 7b). The negative values ΔH°_{ads} and ΔS°_{ads} assume that the inhibitor's adsorption on metal is regarded as an exothermic action and that this is characterized by a reduction in entropy [42].
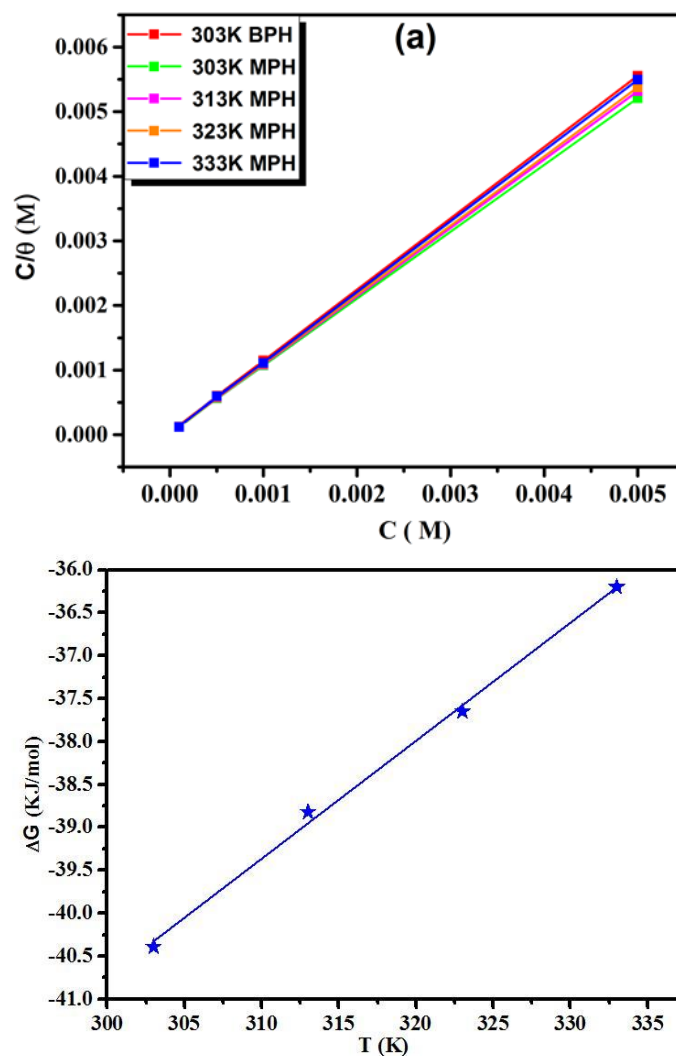

Figure 7. Langmuir adsorption isotherm plots (**a**) and regularity of the standard Gibbs free energy ΔG°_{ads} value of MPH vs. temperature (**b**) on MS in 1.0 M HCl at different temperatures.

Table 9. Thermodynamic parameters of MS corrosion in the presence of MPH and BPH in 1.0 M HCl.

Inhibitor	Temperature (K)	K_{ads} (L mol^{-1})	R^2	$\Delta G^\circ{}_{ads}$ (kJ mol^{-1})	ΔH_a (kJ mol^{-1})	ΔS_a (J mol^{-1} K^{-1})
BPH	303	28,142	0.999	−35.90	-	-
MPH	303	31,588	0.999	−40.39	−81.95	−13.7
	313	34,901	0.999	−38.82		
	323	34,486	0.999	−37.65		
	333	39,347	0.999	−36.20		

3.5. Scanning Electron Microscopy (SEM)/Energy Dispersive Spectroscopy (EDX) Study

With the objective of evaluating the morphology of the metal surface to confirm the corrosion inhibition effectiveness of the tested inhibitors, scanning electron microscopy was performed. Surface morphologies of the studied MS in Figure 8a,b depict the SEM images of the MS being investigated, which were soaked for 24 h in a non-inhibited solution and an inhibited solution with the compound MPH at a concentration of 5×10^{-3} M. In Figure 8a, we observe that the surface shows corrosion and the presence of internal cracks with many depressions and cavities; this is undoubtedly indicative of rapid a corrosion attack in an aggressive environment. Nevertheless, the surface is smoother in the presence of the inhibitor in the guide, as seen in Figure 8b.In order to examine the protection mechanism, EDX analyses of the steel surface were performed after 24 h of immersion in HCl. In this latter medium, the presence of peaks corresponding to oxygen, carbon, and iron were detected by EDX analysis on the MS substrate before the addition of the inhibitor (Figure 8c). By comparing the EDX spectrum of the sample in the presence of MPH with that of the blank, it is clear that the peak of chlorine and oxygen declines in the EDX spectra when MPH is present. Such remarks approve that the MPH compound prevents metal corrosion through the formation of an electrolyte-limiting layer to the metal [15,48]. The presence of nitrogen, aromatic rings and oxygen atoms plays a crucial role in fixing the molecule at the surface, which helps in strengthening its corrosion protection property.
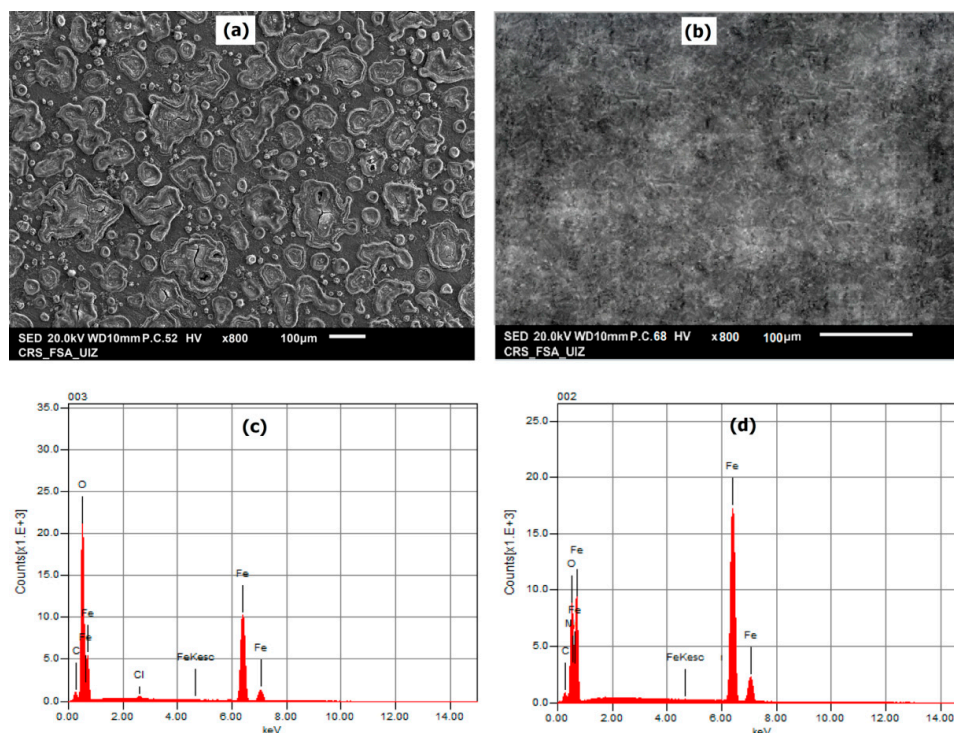
Figure 8. Scanning electron microscopy and energy dispersive spectroscopy images of the MS surface after 24 h immersion in 1.0 M HCl solution in the absence (**a**,**c**) and the presence of 5×10^{-3} M of MPH (**b**,**d**).

4. Conclusions

The corrosion inhibition effects of (E)-N'-(4-bromobenzylidene)-2-(6-methoxynaphthalen-2-yl) propanehydrazide (BPH) and (E)-N'-(4-(dimethylamino) benzylidene)-2-(6-methoxynaphthalen-2-yl) propanehydrazide (MPH) for MS in a solution of 1.0 M HCl were investigated using chemical, electrochemical, and surface characterization techniques. The outcomes clearly show that the increase in the concentration of inhibitors towards an optimal value of 5×10^{-3} M considerably impacted the inhibitory efficacy of the two hydrazone derivatives. Nevertheless, the favorable inhibitory effect of MPH was studied under different temperatures ranging from 303 K to 333 K. However, corrosion inhibition was almost unchanged with increasing immersion time, which implies the long-term stability of the inhibiting effect. It was also concluded from the PDP results that both compounds acted as mixed-type inhibitors with a distinctly cathodic character, and that the adsorption followed the Langmuir isotherm model. The results from SEM analysis confirmed that the MPH compound stopped the corrosion of steel by forming a layer that limits the access of the electrolyte to the surface. The link between the inhibitory effects of the two compounds studied in this work and their molecular structures will be detailed in another article in which we will focus on the theoretical study of hydrazone derivatives reported herein.

References

1. Eddy, N.O.; Ita, B.I. QSAR, DFT and quantum chemical studies on the inhibition potentials of some carbozones for the corrosion of mild steel in HCl. *J. Mol. Model.* **2011**, *17*, 359–376. [CrossRef] [PubMed]

2. Agrawal, A.; Sahu, K. An overview of the recovery of acid from spent acidic solutions from steel and electroplating industries. *J. Hazard. Mater.* **2009**, *171*, 61–75. [CrossRef] [PubMed]

3. Lgaz, H.; Salghi, R.; Ali, I.H. Corrosion inhibition behavior of 9-Hydroxyrisperidone as a green corrosion inhibitor for mild steel in hydrochloric acid: Electrochemical, DFT and MD simulations studies. *Int. J. Electrochem. Sci.* **2018**, *13*, 250–264. [CrossRef]

4. El-Hajjaji, F.; Belghiti, M.E.; Hammouti, B.; Jodeh, S.; Hamed, O.; Lgaz, H.; Salghi, R. Adsorption and corrosion inhibition effect of 2-mercaptobenzimidazole (surfactant) on a carbon steel surface in an acidic medium: Experimental and monte carlo simulations. *Port. Electrochim. Acta* **2018**, *36*, 197–212. [CrossRef]

5. Singh, A.; Ansari, K.R.; Quraishi, M.A.; Lgaz, H. Effect of electron donating functional groups on corrosion inhibition of J55 steel in a sweet corrosive environment: Experimental, density functional theory, and molecular dynamic simulation. *Materials* **2019**, *12*, 17. [CrossRef] [PubMed]

6. Petrunin, M.; Maksaeva, L.; Gladkikh, N.; Makarychev, Y.; Maleeva, M.; Yurasova, T.; Nazarov, A. Thin benzotriazole films for inhibition of carbon steel corrosion in neutral electrolytes. *Coatings* **2020**, *10*, 362. [CrossRef]

7. Odewunmi, N.A.; JafarMazumder, M.A.; Ali, S.A.; Aljeaban, N.A.; Alharbi, B.G.; Al-Saadi, A.A.; Obot, I.B. Impact of degree of hydrophilicity of pyridinium bromide derivatives on HCl pickling of X-60 mild steel: Experimental and theoretical evaluations. *Coatings* **2020**, *10*, 185. [CrossRef]

8. Jawad, Q.A.; Zinad, D.S.; Dawood Salim, R.; Al-Amiery, A.A.; Sumer Gaaz, T.; Takriff, M.S.; Kadhum, A.A.H. Synthesis, characterization, and corrosion inhibition potential of novel thiosemicarbazone on mild steel in sulfuric acid environment. *Coatings* **2019**, *9*, 729. [CrossRef]

9. Hu, J.; Wang, T.; Wang, Z.; Wei, L.; Zhu, J.; Zheng, M.; Chen, Z. Corrosion protection of N80 steel in hydrochloric acid medium using mixed $C_{15}H_{15}NO$ and Na_2WO_4 inhibitors. *Coatings* **2018**, *8*, 315. [CrossRef]

10. Eduok, U.; Ohaeri, E.; Szpunar, J. Electrochemical and surface analyses of X70 steel corrosion in simulated acid pickling medium: Effect of poly (N-vinyl imidazole) grafted carboxymethyl chitosan additive. *Electrochim. Acta* **2018**, *278*, 302–312. [CrossRef]

11. Deyab, M. Corrosion inhibition of heat exchanger tubing material (titanium) in MSF desalination plants in acid cleaning solution using aromatic nitro compounds. *Desalination* **2018**, *439*, 73–79. [CrossRef]

12. Bentiss, F.; Jama, C.; Mernari, B.; El Attari, H.; El Kadi, L.; Lebrini, M.; Traisnel, M.; Lagrenée, M. Corrosion control of mild steel using 3, 5-bis (4-methoxyphenyl)-4-amino-1, 2, 4-triazole in normal hydrochloric acid medium. *Corros. Sci.* **2009**, *51*, 1628–1635. [CrossRef]

13. Glasgow, I.; Rostron, A.; Thomson, G. Hydrogen absorption by very strong steel during chemical descaling. *Corros. Sci.* **1966**, *6*, 469–482. [CrossRef]

14. Soltani, N.; Behpour, M.; Oguzie, E.; Mahluji, M.; Ghasemzadeh, M. Pyrimidine-2-thione derivatives as corrosion inhibitors for mild steel in acidic environments. *RSC Adv.* **2015**, *5*, 11145–11162. [CrossRef]

15. Singh, P.; Srivastava, V.; Quraishi, M. Novel quinoline derivatives as green corrosion inhibitors for mild steel in acidic medium: Electrochemical, SEM, AFM, and XPS studies. *J. Mol. Liq.* **2016**, *216*, 164–173. [CrossRef]

16. Yüce, A.O.; Mert, B.D.; Kardaş, G.; Yazıcı, B. Electrochemical and quantum chemical studies of 2-amino-4-methyl-thiazole as corrosion inhibitor for mild steel in HCl solution. *Corros. Sci.* **2014**, *83*, 310–316. [CrossRef]

17. Al-Sehemi, A.G.; Irfan, A.; Alfaifi, M.; Fouda, A.M.; El-Gogary, T.M.; Ibrahim, D.A. Computational study and in vitro evaluation of the anti-proliferative activity of novel naproxen derivatives. *J. King Saud Univ. Sci.* **2017**, *29*, 311–319. [CrossRef]

18. Almasirad, A.; Tajik, M.; Bakhtiari, D.; Shafiee, A.; Abdollahi, M.; Zamani, M.J.; Khorasani, R.; Esmaily, H. Synthesis and analgesic activity of N-arylhydrazone derivatives of mefenamic acid. *J. Pharm. Pharm. Sci.* **2005**, *8*, 419–425.

19. Rakha, T.; El-Gammal, O.; Metwally, H.; El-Reash, G.A. Synthesis, characterization, DFT and biological studies of (Z)-N′-(2-oxoindolin-3-ylidene) picolinohydrazide and its Co (II), Ni (II) and Cu (II) complexes. *J. Mol. Struct.* **2014**, *1062*, 96–109. [CrossRef]

20. Rollas, S.; Küçükgüzel, S.G. Biological activities of hydrazone derivatives. *Molecules* **2007**, *12*, 1910–1939. [CrossRef]

21. Albayati, M.R.; Kansız, S.; Dege, N.; Kaya, S.; Marzouki, R.; Lgaz, H.; Salghi, R.; Ali, I.H.; Alghamdi, M.M.; Chung, I.-M. Synthesis, crystal structure, Hirshfeld surface analysis and DFT calculations of 2-[(2, 3-dimethylphenyl) amino]-N′-[(E)-thiophen-2-ylmethylidene] benzohydrazide. *J. Mol. Struct.* **2020**, *1205*, 127654. [CrossRef]

22. Mohamad, A.D.M.; Abualreish, M.; Abu-Dief, A.M. Antimicrobial and anticancer activities of cobalt (III)-hydrazone complexes: Solubilities and chemical potentials of transfer in different organic co-solvent-water mixtures. *J. Mol. Liq.* **2019**, *290*, 111162. [CrossRef]

23. Lgaz, H.; Chaouiki, A.; Albayati, M.R.; Salghi, R.; El Aoufir, Y.; Ali, I.H.; Khan, M.I.; Mohamed, S.K.; Chung, I.-M. Synthesis and evaluation of some new hydrazones as corrosion inhibitors for mild steel in acidic media. *Res. Chem. Intermed.* **2019**, *45*, 2269–2286. [CrossRef]

24. Lgaz, H.; Chung, I.-M.; Albayati, M.R.; Chaouiki, A.; Salghi, R.; Mohamed, S.K. Improved corrosion resistance of mild steel in acidic solution by hydrazone derivatives: An experimental and computational study. *Arab. J. Chem.* **2020**, *13*, 2934–2954. [CrossRef]

25. Lgaz, H.; Zehra, S.; Albayati, M.R.; Toumiat, K.; El Aoufir, Y.; Chaouiki, A.; Salghi, R.; Ali, I.H.; Khan, M.I.; Chung, I.-M.; et al. Corrosion inhibition of mild steel in 1.0 M HCl by two hydrazone derivatives. *Int. J. Electrochem. Sci.* **2019**, *14*, 6667–6681. [CrossRef]

26. ASTM, G 31–72. American Society for Testing and Materials Philadelphia, PA. 1990.—Recherche Google. Available online: https://www.google.com/search?q=ASTM%2C+G+31%E2%80%9372%2C+American+Society+for+Testing+and+Materials+Philadelphia%2C+PA%2C+1990.&oq=ASTM%2C+G+31%E2%80%9372%2C+American+Society+for+Testing+and+Materials+Philadelphia%2C+PA%2C+1990.&aqs=chrome..69i57j69i60.4733j0j7&sourceid=chrome&ie=UTF-8 (accessed on 20 March 2019).

27. Haynes, G. Review of laboratory corrosion tests and standards. In *Corrosion Testing and Evaluation: Silver Anniversary Volume*; ASTM International: West Conshohocken, PA, USA, 1990.

28. Salghi, R.; Jodeh, S.; Ebenso, E.E.; Lgaz, H.; Ben Hmamou, D.; Belkhaouda, M.; Ali, I.H.; Messali, M.; Hammouti, B.; Fattouch, S. Inhibition of C-steel corrosion by green tea extract in hydrochloric solution. *Int. J. Electrochem. Sci.* **2017**, *12*, 3283–3295. [CrossRef]

29. Bouoidina, A.; El-Hajjaji, F.; Drissi, M.; Taleb, M.; Hammouti, B.; Chung, I.-M.; Jodeh, S.; Lgaz, H. Towards a deeper understanding of the anticorrosive properties of hydrazine derivatives in acid medium: Experimental, DFT and MD simulation assessment. *Metall. Mater. Trans. A* **2018**, *49*, 5180–5191. [CrossRef]

30. Bashir, S.; Sharma, V.; Lgaz, H.; Chung, I.-M.; Singh, A.; Kumar, A. The inhibition action of analgin on the corrosion of mild steel in acidic medium: A combined theoretical and experimental approach. *J. Mol. Liq.* **2018**, *263*, 454–462. [CrossRef]

31. Tezcan, F.; Yerlikaya, G.; Mahmood, A.; Kardaş, G. A novel thiophene Schiff base as an efficient corrosion inhibitor for mild steel in 1.0 M HCl: Electrochemical and quantum chemical studies. *J. Mol. Liq.* **2018**, *269*, 398–406. [CrossRef]

32. Singh, A.K.; Ebenso, E.E.; Quraishi, M. Adsorption behaviour of cefapirin on mild steel in hydrochloric acid solution. *Int. J. Electrochem. Sci.* **2012**, *7*, 2320.

33. Bentiss, F.; Gassama, F.; Barbry, D.; Gengembre, L.; Vezin, H.; Lagrenée, M.; Traisnel, M. Enhanced corrosion resistance of mild steel in molar hydrochloric acid solution by 1, 4-bis (2-pyridyl)-5H-pyridazino [4, 5-b] indole: Electrochemical, theoretical and XPS studies. *Appl. Surf. Sci.* **2006**, *252*, 2684–2691. [CrossRef]

34. Chakravarthy, M.; Mohana, K.; Kumar, C.P. Corrosion inhibition effect and adsorption behaviour of nicotinamide derivatives on mild steel in hydrochloric acid solution. *Int. J. Ind. Chem.* **2014**, *5*, 19. [CrossRef]

35. Shukla, S.K.; Quraishi, M. 4-Substituted anilinomethylpropionate: New and efficient corrosion inhibitors for mild steel in hydrochloric acid solution. *Corros. Sci.* **2009**, *51*, 1990–1997. [CrossRef]

36. Chen, W.; Hong, S.; Xiang, B.; Luo, H.; Li, M.; Li, N. Corrosion inhibition of copper in hydrochloric acid by coverage with trithiocyanuric acid self-assembled monolayers. *Corros. Eng. Sci. Technol.* **2013**, *48*, 98–107. [CrossRef]

37. Solmaz, R. Investigation of the inhibition effect of 5-((E)-4-phenylbuta-1, 3-dienylideneamino)-1, 3, 4-thiadiazole-2-thiol Schiff base on mild steel corrosion in hydrochloric acid. *Corros. Sci.* **2010**, *52*, 3321–3330. [CrossRef]

38. Njoku, D.I.; Li, Y.; Lgaz, H.; Oguzie, E.E. Dispersive adsorption of Xylopiaaethiopica constituents on carbon steel in acid-chloride medium: A combined experimental and theoretical approach. *J. Mol. Liq.* **2018**, *249*, 371–388. [CrossRef]

39. Bousskri, A.; Anejjar, A.; Messali, M.; Salghi, R.; Benali, O.; Karzazi, Y.; Jodeh, S.; Zougagh, M.; Ebenso, E.E.; Hammouti, B. Corrosion inhibition of carbon steel in aggressive acidic media with 1-(2-(4-chlorophenyl)-2-oxoethyl) pyridazinium bromide. *J. Mol. Liq.* **2015**, *211*, 1000–1008. [CrossRef]

40. Obot, I.; Obi-Egbedi, N.; Ebenso, E.; Afolabi, A.; Oguzie, E. Experimental, quantum chemical calculations, and molecular dynamic simulations insight into the corrosion inhibition properties of 2-(6-methylpyridin-2-yl) oxazolo [5, 4-f][1, 10] phenanthroline on mild steel. *Res. Chem. Intermed.* **2013**, *39*, 1927–1948. [CrossRef]

41. Belghiti, M.E.; Tighadouini, S.; Karzazi, Y.; Dafali, A.; Hammouti, B.; Radi, S.; Solmaz, R. New hydrazine derivatives as corrosion inhibitors for mild steel protection in phosphoric acid medium. Part A: Experimental study. *J. Mater. Env. Sci. 2016a* **2007**, *7*, 337–346.

42. Umoren, S.A.; Eduok, U.M.; Solomon, M.M.; Udoh, A.P. Corrosion inhibition by leaves and stem extracts of Sidaacuta for mild steel in 1 M H_2SO_4 solutions investigated by chemical and spectroscopic techniques. *Arab. J. Chem.* **2016**, *9*, S209–S224. [CrossRef]

43. Myung, N.V.; Park, D.-Y.; Yoo, B.-Y.; Sumodjo, P.T. Development of electroplated magnetic materials for MEMS. *J. Magn. Magn. Mater.* **2003**, *265*, 189–198. [CrossRef]

44. Li, X.; Deng, S.; Lin, T.; Xie, X.; Du, G. 2-Mercaptopyrimidine as an effective inhibitor for the corrosion of cold rolled steel in HNO_3 solution. *Corros. Sci.* **2017**, *118*, 202–216. [CrossRef]

45. Aljourani, J.; Raeissi, K.; Golozar, M. Benzimidazole and its derivatives as corrosion inhibitors for mild steel in 1M HCl solution. *Corros. Sci.* **2009**, *51*, 1836–1843. [CrossRef]

46. Gurudatt, D.M.; Mohana, K.N. Synthesis of new pyridine based 1, 3, 4-oxadiazole derivatives and their corrosion inhibition performance on mild steel in 0.5 M hydrochloric acid. *Ind. Eng. Chem. Res.* **2014**, *53*, 2092–2105. [CrossRef]

47. Mahdavian, M.; Ashhari, S. Corrosion inhibition performance of 2-mercaptobenzimidazole and 2-mercaptobenzoxazole compounds for protection of mild steel in hydrochloric acid solution. *Electrochim. Acta* **2010**, *55*, 1720–1724. [CrossRef]

48. Revilla, R.I.; Liang, J.; Godet, S.; De Graeve, I. Local corrosion behavior of additive manufactured AlSiMg alloy assessed by SEM and SKPFM. *J. Electrochem. Soc.* **2017**, *164*, C27–C35. [CrossRef]